MULTIPHYSICS AND PRESSURE CODE ANALYSIS FOR QUARTER WAVE β=0.085 AND HALF WAVE β=0.29 RESONATORS*

S. Miller#, M. Johnson, A Facco, Y. Xu, J. Binkowski,
Facility For Rare Isotope Beams, Michigan State University, MI 48824, USA

Abstract

The driver linac design for the Facility for Rare Isotope Beams (*FRIB*) at Michigan State University (*MSU*) makes use of four optimized superconducting radio frequency (*RF*) resonators to accelerate exotic ions to 200 MeV/μ. The RF resonators were optimized using computer simulations for all expected physical encounters and corresponding electrical resonant frequency changes. Principal guidance from the ASME boiler and pressure vessel code (BPVC) were applied.

INTRODUCTION

The FRIB, a new national user facility funded by the U.S. Department of Energy Office of Science to be constructed and operated by MSU, is currently being designed to provide intense beams of rare isotopes to better understand the physics of nuclei, nuclear astrophysics, fundamental interactions, and applications for society. The FRIB driver accelerator can accelerate all stable isotopes to energies beyond 200 MeV/u at beam powers up to 400 kW [1]. FRIB uses two *80.5 MHz λ/4* quarter wavelength resonators (*QWR*) operate at $\beta_{opt} = v/c = 0.041$ and *0.085* and two *322 MHz λ/2* half wavelength resonators (*HWR*) operate at $\beta_{opt} = 0.29$ and *0.53*; Figure 1.

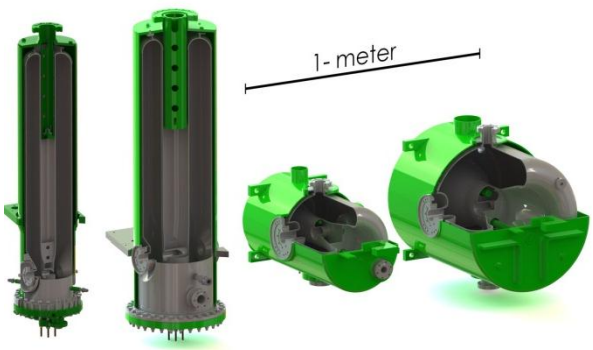

Figure 1: The FRIB Resonators. From left to right: 80.5 MHz β = 0.041, 80.5 MHz β = 0.085, 322 MHz, β = 0.29, 322 MHz β = 0.53.

INTEGRATED ANALYSIS APPROACH

Project requirements state resonator designs must satisfy BPVC. The analysis for the 80.5 MHz β = 0.041 has been completed and was presented at SRF2009 [2]. For the remaining 3 resonators, the first step of the analysis was to validate the design using equivalence of the ASME Section VIII, Division 2. This analysis[3] yields pressure capability for 300K and 2K. Table 1 displays the material allowable stresses as established by ASME code, and the Table 2 displays the stress states that exist during the pressurization of the helium vessel. P_m is the general membrane stress allowable, P_l is the local membrane stress allowable, and $P_l + P_b$ is the local plus the bending stress allowable.

Table 1: Resonator Material Properties [4], [5], [6]

Material	Temp (K)	Elastic Modulus (GPa)	Yield Strength (MPa)
Niobium RRR250	295	103.0	38
Niobium RRR250	4	104.0	372
Niobium-45 Titanium	295	62.1	475
Niobium-45 Titanium	4	68.2	680
Grade 2 Titanium	295	106.9	275
Grade 2 Titanium	4	118.8	560

Table 2: Resonator Stress Allowable [4], [5], [6]

Material	Temp (K)	Pm (MPa)	Pl (MPa)	Pl + Pb (MPa)
Niobium RRR250	295	25	38	38
Niobium RRR250	4	248	372	372
Niobium-45 Titanium	295	226	340	340
Niobium-45 Titanium	4	450	680	680
Grade 2 Titanium	295	143	214	214
Grade 2 Titanium	4	375	560	560

The second step verified the resonator tuning sensitivity, tuning range, and tuning force. The simulation was also used to determine maximum stresses in the resonator and stiffen the resonator as needed to achieve the required tuning range.

The next step of the integrated approach was to determine the resonators helium pressure sensitivity. If the pressure sensitivity was found to be too high, stiffeners were added accordingly.

The final step of the integrated analysis was to compute the Lorentz Force Detuning (LFD). The LFD value was compared to the target goal and if too high design changes were necessary.

*Work supported by US DOE Cooperative Agreement DE-SC000061
#millers@frib.msu.edu

Requirements

The four resonator types share a common set of mechanical requirements:

- Satisfy Elastic Stress Analysis Method at 2.0 ATM for 300K
- Capable of sustaining tuning stresses generated at maximum tuning range and pressure
- Pressure sensitivity between +/-4Hz/torr
- LFD >-4Hz/(MV-m)^2

Quarter Wave Resonator

The β=0.085 resonator (shown in Figure 2 with labels) underwent pressure simulation. The first step of the process was to apply stress classification lines (SCLs) to the expected high stress areas of the resonator. Figure 3 display the stress line locations on the β=0.085 resonator. High stress regions on this resonator are predominantly interface points. These include the short plate to inner conductor interface, short plate to outer conductor interface. Other areas include port interface to the outer conductor and the helium vessel.

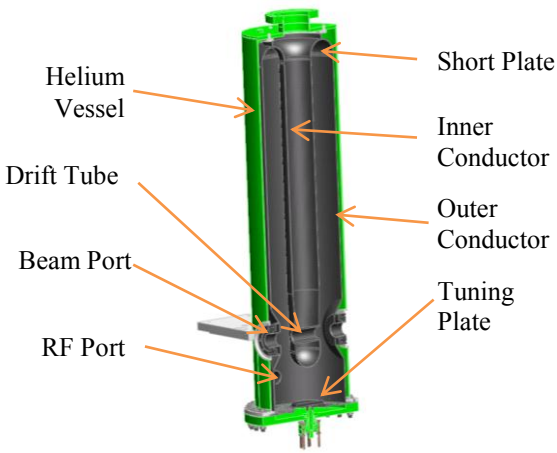

Figure 2: Labeled β=0.085 Resonator.

The next step in the pressure simulation was to apply pressure to the interior surface on the helium vessel and the exterior surfaces of the cavity. Figure 3 displays the pressure areas of the β=0.085 resonator.

After the pressure has been applied, the stress at each of the SCLs is evaluated. The pressure is increased until one of the SCLs exceeds the limits established by the Elastic Stress Analysis Method for 300K and 2K material properties. The last point where the SCL satisfies the Elastic Stress Analysis Method establishes the pressure capability at the material properties temperature. The β=0.085 resonator design achieved a 300K pressure capability of 2.2 ATM and a 2K pressure capability of 15 ATM. Figure 4 displays the equivalent stress plot at a high stress location near the beam port at 300K. Figure 5 shows its corresponding SCL plot through the wall thickness.

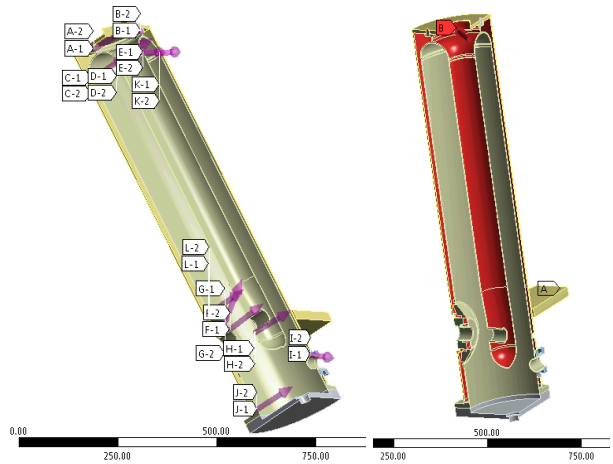

Figure 3: β=0.085 Resonator Stress Line Locations and Resonator Boundary Conditions (Pressure Area in Red).

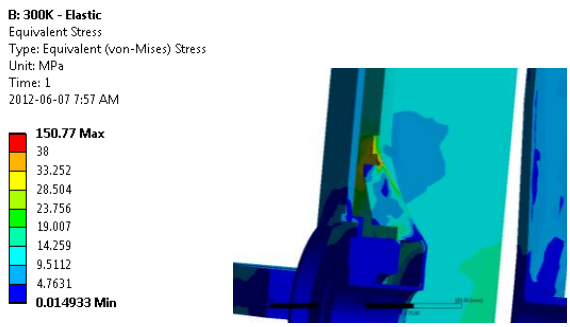

Figure 4: β=0.085 Resonator High Stress Location.

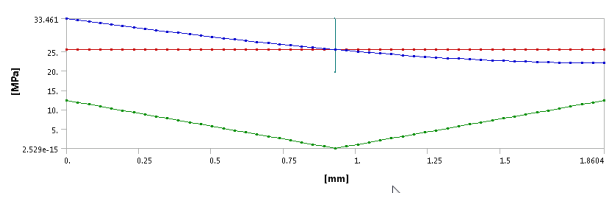

Figure 5: β=0.085 Resonator SCL Result (Pm=Red, Pb=Green, Pl+Pb=Blue).

The next phase of integrated testing was to find the tuning parameters for the β=0.085 resonator. The first step of this process was to find the tuning sensitivity. On the β=0.085 resonator, a tuning plate is present on the bottom of the resonator (See Figure 2) and is actuated inwards and outwards to adjust the frequency. This adjustment results in 3.2 kHz/mm shift on the resonator. With a tuning range of +/- 10 kHz required for this resonator, this requires 3.125 mm of adjustment, inward and outward. Figure 6 displays the stress generated on tuning plate at 4 mm upward adjustment at 2K, the temperature at which tuning would takes place. The tuning plate is capable of the required tuning range without yield through its thickness.

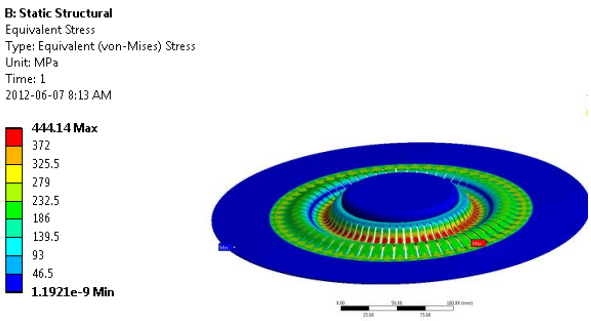

Figure 6: β=0.085 Resonator Tuning Plate Stress.

The third step of integrated analysis was to find the pressure sensitivity. This was performed by applying pressure (1 ATM) to the same surfaces shown in Figure 3, and simulating the frequency shift due to this pressure. Figure 7 displays the deformation due to the pressure application, this deformation results in a -1.4 Hz/torr frequency shift. This falls within the requirement for pressure sensitivity.

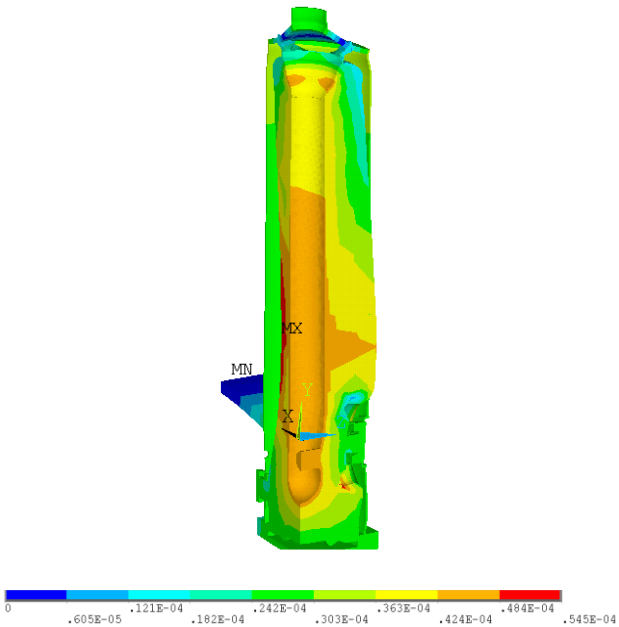

Figure 7: β=0.085 Resonator Helium Pressure Response.

The last step of the integrated analysis for the β=0.085 was to compute the LFD value. This simulation used the same model as the pressure sensitivity; however, instead of pressure loads being added, Lorentz Forces are computed and applied to the model. In the same fashion as the pressure sensitivity, the frequency shift is determined due to this force. Figure 8 depicts the deformed shape of the β=0.085 resonator due the Lorentz Force. This plots displays the high electric field regions pulling towards each other, predominantly on the beam port and drift tube areas. Conversely, the magnetic field regions are pushing outward. From this plot it was found the LFD value for this resonator was -0.7 Hz/(MV-m)^2. This meets the goal of being greater than –4 Hz/(MV-m)^2.

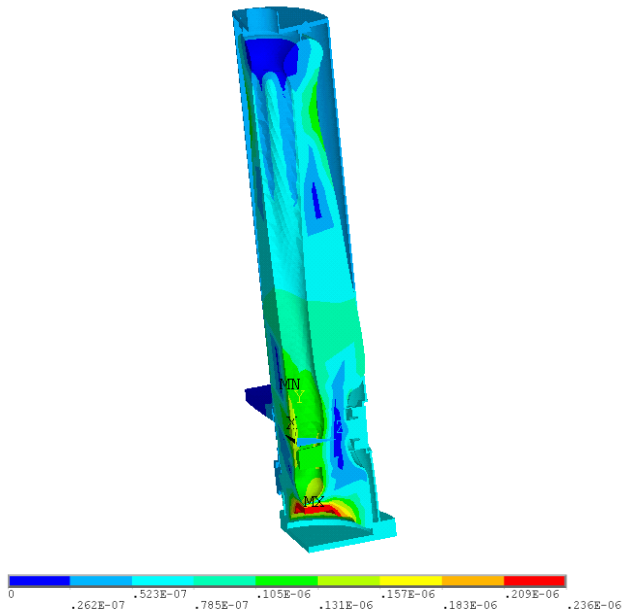

Figure 8: β=0.085 Resonator LFD Response.

Half Wave Resonator

The β=0.29 resonator (shown in Figure 9 with labels) underwent pressure simulation. The first step of the process was to apply stress classification lines (SCLs) to the expected high stress areas of the resonator. Figure 10 displays the stress line locations on the β=0.29 resonator. High stress regions on this resonator are predominantly interface points. These include the short plate to inner conductor interface, short plate to outer conductor interface. Other areas include port interface to the outer conductor and the helium vessel.

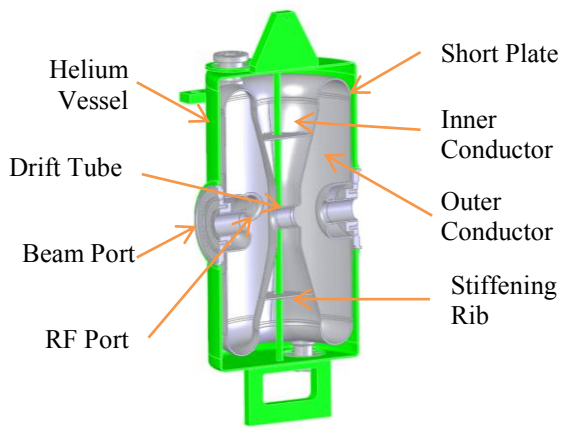

Figure 9: β=0.29 Labeled Resonator.

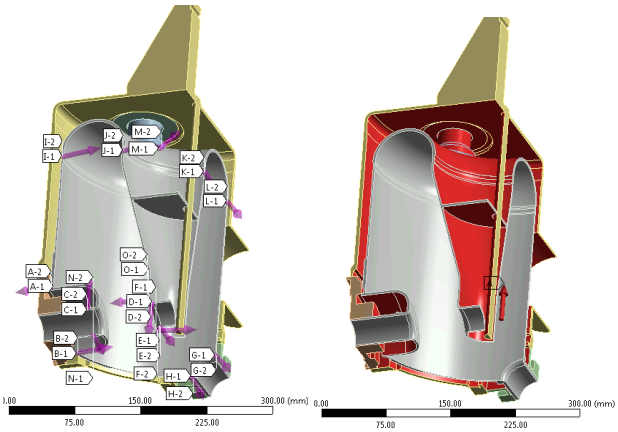

Figure 10: β=0.29 Resonator Stress Line Locations and Resonator Boundary Conditions (Pressure Area in Red).

The next step in the pressure simulation was to apply pressure to the interior surface on the helium vessel and the exterior surfaces of the cavity. Figure 10 displays the pressure areas of the β=0.29 resonator.

After the pressure has been applied, the stress at each of the stress lines is evaluated. The pressure is increased until one of the SCLs exceeds the limits established by the Elastic Stress Analysis Method for 300K and 2K material properties. The last point where the SCL satisfies the Elastic Stress Analysis Method establishes the pressure capability at the material properties temperature. The β=0.29 resonator design achieved a 300K pressure capability of 2.2 ATM and 2K pressure capability of 20 ATM. Figure 11 display the equivalent stress plot at a high stress location for 300K and Figure 12 shows its corresponding SCL plot through the wall thickness.

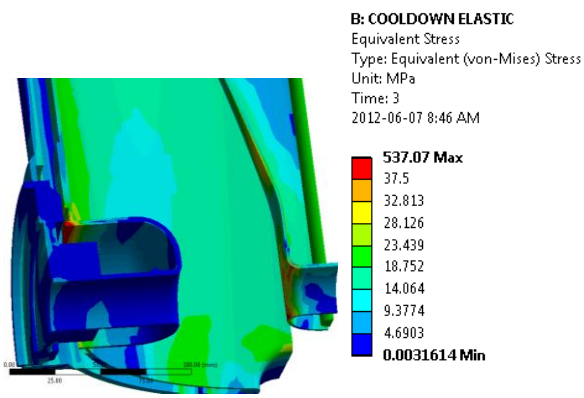

Figure 11: β=0.29 Resonator High Stress Location.

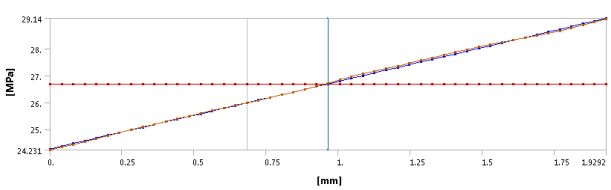

Figure 12: β=0.29 Resonator SCL Result (Pm=Red, Pb=Green, Pl+Pb=Blue).

The next phase of integrated testing was to find the tuning parameters for the β=0.29 resonator. The first step of this process was to find the tuning sensitivity. On the β=0.29 resonator, the beam port flanges on the resonator are actuated inwards to adjust the frequency. This adjustment results in 216.5 kHz/mm shift on the resonator. With a tuning range of +/- 120 kHz required for this resonator, this necessitates .554 mm of flange to flange adjustment inward. Figure 13 display the stress generated on the resonator at .554 mm of adjustment at 2K. This figure displays that the resonator is capable of the required tuning range, since there is not yielding present due to the tuning deflection and pressure.

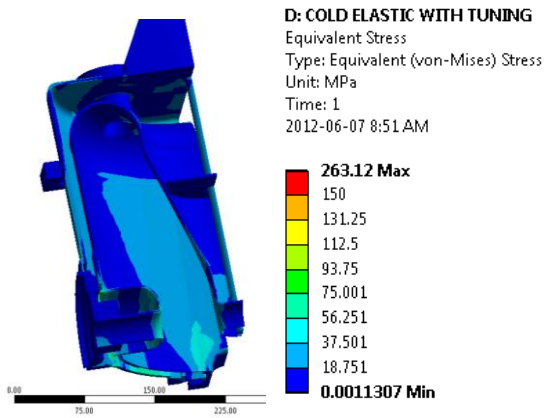

Figure 13: β=0.29 Resonator stresses during maximum tuning.

The third step of integrated analysis is to find the pressure sensitivity. This was performed by applying pressure (1 ATM) to the same surfaces shown in Figure 10, and simulating the frequency shift due to this pressure. Two scenarios were simulated, one where the beam port flanges are fixed (representing and ideal tuner) and the other where the beam port flanges are free. The two scenarios help define the resonator's overall pressure sensitivity due to the tuner. The tuner will have a finite rigidity that is somewhere between the fixed and free condition. Figure 14 displays the deformation due to the pressure application at the fixed condition, this deformation results in a 0.55 Hz/torr frequency shift. At the free condition, the pressure sensitivity is 1.42 Hz/torr. Both of these conditions fall within the requirement for pressure sensitivity, which demonstrates that the resonator's pressure sensitivity can meet its requirement independent of the tuner.

A study was performed on the β=0.29 Resonator, to find the ideal location of the stiffening ribs (Figure 9). By moving the rib up and down on the inner conductor, the pressure sensitivity could be altered. The rib was finally placed at the location (185.75 mm above and below the drift tube) that results in the 0.55 Hz/torr frequency shift at the fixed condition. Figure 15 displays the results of this study.

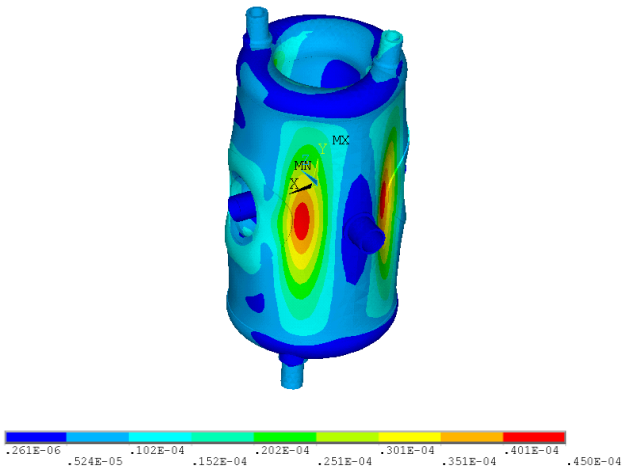

Figure 14: β=0.29 Resonator Helium Pressure Response.

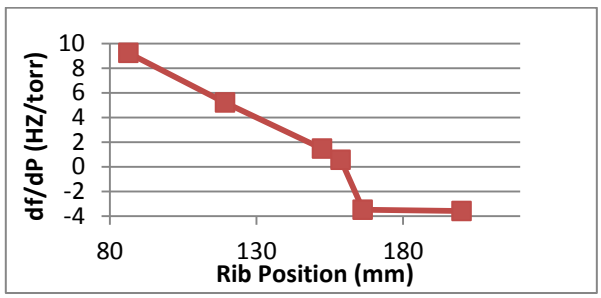

Figure 15: β=0.29 Resonator Stiffening Rib Study.

The last step of the integrated analysis for the β=0.29 was to compute the LFD value. This simulation used the same model as the pressure sensitivity; however, instead of pressure loads being added, Lorentz Forces are computed and applied to the model. In the same fashion as the pressure sensitivity, the frequency shift is determined due to this force. Like the pressure sensitivity, two scenarios were simulated; one with beam ports fixed and the other with beam ports free (representing an ideal tuner and no tuner respectively). Figure 16 depicts the deformed shape of the β=0.29 resonator due the Lorentz Force at the fixed condition. This plots displays the high electric field regions pulling towards each other, predominantly on the beam port and drift tube areas. Conversely the magnetic field regions are pushing outward. From this figure, it was found the LFD value for the resonator at the fixed condition was -2.71 Hz/(MV-m)^2. At the free condition, the value is -3.72 Hz/(MV-m)^2. Both conditions meet the requirement for LFD, demonstrating that the resonator can achieve its requirement independent of the tuner.

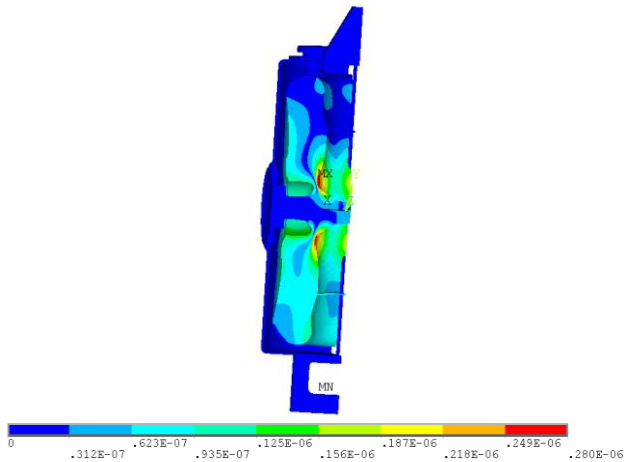

Figure 16: β=0.29 Resonator LFD Response.

CONCLUSION

Property	β=0.085	β=0.29
Pressure Capability 300K (ATM)	2.2	2.2
Pressure Capability 2K (ATM)	15	20
Tuning Sensitivity (kHz/mm)	3.2	216.5
Pressure Sensitivity (Hz/torr) Fixed Tuner	N/A	0.55
Pressure Sensitivity (Hz/torr) Free Tuner	-1.4	1.42
LFD (Hz/(MV/m)^2 Fixed Tuner	N/A	-2.71
LFD (Hz/(MV/m)^2 Free Tuner	-0.7	-3.72

Table 3 summarizes the resonators mechanical attributes. The integrated mechanical analysis of the β=0.29 and β=0.085 resonator types at FRIB is complete. The β=0.29 half wave resonator has completed the analysis and has been shown to exceed the mechanical requirements. This resonator type has already undergone the request for quote process and two development resonators are expected by the end of 2012. The β=0.085 resonator has also completed its integrated mechanical analysis and exceeds the mechanical requirements. This resonator has also completed a request for quote process and two development resonators of this type are expected by the end of 2012.

REFERENCES

[1] J.Wei et al., "The FRIB Project – Accelerator Challenges and Progress", these proceedings.
[2] E. Zaplatin et al., "Structural Analyses of MSU Quarter-Wave Resonators". SRF 2009: Berlin, Germany.
[3] ANSYS, Inc., Cannonsburg, Pennsylvania, USA.
[4] T.J. Peterson et al., "Pure Niobium as a Pressure Vessel Material," Fermi National Accelerator Laboratory, Batavia, IL, USA.
[5] ASME Boiler and Pressure Vessel Code, 2010 edition.
[6] ATI Wah Chang, Technical Data for Niobium-Titanium, 2011.